frontiers in Earth Science

ORIGINAL RESEARCH
published: 28 October 2021
doi: 10.3389/feart.2021.736598

Reservoir Characteristics and Controlling Factors of Oil Content in Hybrid Sedimentary Rocks of the Lucaogou Formation, Western Jimusar Sag, Junggar Basin

Haitao Xue, Ce An, Zhentao Dong, Dianshi Xiao, Jinliang Yan, Guozhi Ding, Penglei Yan and Jinxu Zhang*

Shandong Provincial Key Laboratory of Deep Oil and Gas, China University of Petroleum (East China), Qingdao, China

Hybrid sedimentary rocks (HSR) are a major reservoir type in unconventional oil exploration. The reservoir characteristics and controlling factors of the oil content of HSR are not clear, restricting the understanding of the storage mechanism and sweet spots within HSR. The Lucaogou Formation in the western Jimusar Sag is taken as a case study. Starting with the classification of the lithofacies system, differences in the microscopic pore structure, oil content and controlling factors of HSR reservoirs are revealed. The results show that seven lithofacies are recognized based on mineral composition, sedimentary structure, and organic matter characteristics, exhibiting rapid vertical and horizontal changes affected by the sedimentary environment. Layered mudstone lithofacies of the shallow lake mud and massive dolomitic mudstone lithofacies of dolomitic mud flats have the worst physical properties and oil content properties. However, they do have high organic matter contents and are the main source rocks of the Lucaogou Formation. The massive argillaceous siltstone and massive argillaceous dolomite lithofacies interbed frequently. Although their physical properties are moderate, "source-reservoir integrated" unconventional oil reservoirs can be formed, due to the adjacent to the source rock. Massive dolomitic siltstone, massive siltstone, and massive silty dolomite lithofacies are developed in the middle of the Lucaogou Formation, with the highest proportion of mesopores and macropores, which is indicative of good storage properties. When these lithofacies are filled with crude oil generated from source rocks at the top and bottom of the formation, "source storage adjacent" unconventional oil reservoirs be formed. The oil content is also controlled by the pore structure and specific surface area. The proportion of macropores and mesopores is positively correlated with oil content. The oil content of the samples is very low, when the specific surface area exceeds 2 m^2/g. This manuscript provides a geological basis for evaluating and establishing reasonable interpretation models of HSR sweet spots.

Keywords: hybrid sedimentary rocks, lithofacies type, reservoir properties, factors affecting oil content, lucaogou formation

OPEN ACCESS

Edited by:
Guochang Wang,
Saint Francis University, United States

Reviewed by:
Fahad Ali,
Bacha Khan University, Pakistan
Charles Makoundi,
University of Tasmania, Australia
Enze Wang,
Peking University, China

****Correspondence:***
Zhentao Dong
dzt5020@qq.com

Specialty section:
This article was submitted to Economic Geology, a section of the journal Frontiers in Earth Science

Received: *05 July 2021*
Accepted: *01 October 2021*
Published: *28 October 2021*

Citation:
Xue H, An C, Dong Z, Xiao D, Yan J, Ding G, Yan P and Zhang J (2021) Reservoir Characteristics and Controlling Factors of Oil Content in Hybrid Sedimentary Rocks of the Lucaogou Formation, Western Jimusar Sag, Junggar Basin. Front. Earth Sci. 9:736598. doi: 10.3389/feart.2021.736598

1 INTRODUCTION

In recent years, excellent examples of resource potential from the Lucaogou Formation have researchers to focus on the reservoir characteristics of this lacustrine deep-water sedimentary (Hu et al., 2018; Pang et al., 2018; Yang et al., 2018). Hybrid sedimentary rocks (HSR) are the result of multi-source mixed accumulation Mount (1984), such as clastic sediments, chemical sediments and volcanism. It has the characteristics of fine-grained sedimentation, diverse lithofacies, and frequent interbeds (Li et al., 2015). Although breakthroughs have been made in exploring marine shale, scholars are continuing to make progress in the deposition, structure, and distribution characteristics (Schieber, 1990; Plint et al., 2012). HSR exploration and development still have uncertainties, such as their lithofacies type, pore structure description, and oil evaluation.

The key factor affecting the resource potential of the HSR is considered to be the heterogeneity of lithofacies (Cao et al., 2017a). Lithofacies is a synthesis of various petrological information. Lithofacies represents the sedimentary environment (Liu et al., 2019). Previous studies have resulted in a large number of lithofacies classification of marine shale (Zhao et al., 2016; Zhang et al., 2018). Most studies used mineral composition, structure, and organic matter content as the standard for classification of lithofacies. At present, there is a lack of systematic research on lithofacies changes, because the Lucaogou Formation has been considered as a high-quality source rock before.

The pore size of porous medium classification proposed by International Union of Pure and Applied Chemistry (IUPAC) was generally accepted for chemical products and coal in 1972. Specifically, the pores were divided based on diameter into micropores (<2 nm), mesopores (2–50 nm), and macropores (>50 nm) Everett (1972). This classification standard may be more suitable for chemical products (Zhang et al., 2017), but it has poor application for HSR reservoirs. Because the pores in HSR reservoirs are different, specifically their size of chemical products and coal, the pores are generally between a few nanometers and hundreds of nanometers (Lu et al., 2018). The IUPAC classification scheme is too small for HSR reservoirs (Loucks et al., 2012), and we should establish a suitable pore size classification scheme. Previous scholars have used various experimental methods to reveal the pore system of HSR. This included low-temperature nitrogen adsorption/desorption (Wang and Ju 2015), mercury intrusion capillary pressure(MICP) (Clarkson et al., 2013), low-field nuclear magnetic resonance (NMR) (Zeng et al., 2021b), field emission scanning electron microscopy (FE-SEM) (Tian et al., 2013), computed tomography (CT) (Guo et al., 2015). In addition, Photoshop, ImageJ, and SEM combined with fractal theory to obtain pore images can also be used to quantitatively evaluate porosity distribution and pore size classification (Tian et al., 2021). Low-temperature nitrogen adsorption/desorption can only reveal pore spaces <50 nm and cannot describe the pore space of the reservoir on a large scale (Zeng et al., 2021a). FE-SEM and CT directly reflect the size and shape of the pores but cannot describe the distribution of the reservoir pores and the pore throats. MICP is commonly used to characterize pores greater than 50 nm in diameter. Among the above techniques, MICP combined with fractal theory (He and Hua 1988) are worth employing to reveal the relationship between pore throat size and pore throat combination and can effectively reveal the pore structure (Li et al., 2013).

Oil content is a crucial parameter of HSR reservoirs, and its content represents production output (Zou et al., 2014; He et al., 2018). Previous scholars used experimental methods such as rock pyrolysis, solvent extraction, vapor adsorption, and solid-liquid adsorption to document the conventional parameters TOC, S_1, and OSI index (S_1/TOC × 100) (Wang et al., 2020), to indirectly reflect the oil content in the reservoir (Jarvie, 2012; Wang et al., 2021). However, the above methods have shortcoming. These experiments destroy the sample's integrity, affect the calculation of the oil content, and do not directly reveal the oil content of the reservoir (Jiang et al., 2016). Nuclear magnetic resonance (NMR) technology maintains the sample's integrity and has been widely used in reservoir characterization, to detect the porosity, permeability, pore size distribution (Li et al., 2019), and even the wettability (Odusina et al., 2011) of the reservoir. Two-dimensional nuclear magnetic resonance (2D-NMR) was also used to reflect different fluid types (Li et al., 2020). For example, the oil, water, and solid organic matter content can be obtained through 2D-NMR. In addition, although quantitative grain fluorescence on extract (QGF-E) technology has been applied in oil and gas exploration for more than 100 years, it was not widely used in oil exploration until the 1950s (Liu and Eadington 2005). QGF-E is a low-cost technology for the petroleum industry, which is used to detect ancient oil reservoirs and residual oil. In conventional oil reservoirs, QGF-E has been widely used to study oil and gas changes and their migration history. Nevertheless, it is relatively less used in the evaluation of oil-bearing properties of HSR reservoirs. QGF-E technology characterized by low sample requirements, a low cost, reduced time, and high sensitivity (Liu et al., 2019). The enrichment of crude oil is always a major issue of interest to scholars (Song et al., 2021). The enrichment mode of tight oil can be divided into source-reservoir interlayer type (Chang 7 Member of the Ordos Basin) and shale type (Qingshankou Formation in the Songliao Basin). However, there are relatively few studies on the HSR (Jiao et al., 2020). However, there are relatively few studies on the HSR.

Previous research on Jimusar was limited to the eastern slope area. We selected three typical wells in the western sag as the research area, in response to the call for no restricted areas for exploration. In this study, the main lithologies were determined through thin section identification and x-ray diffraction. The pore structural characteristics of the HSR reservoir were studied by MICP and SEM. The oil contents were analyzed by QGF-E and 2D-NMR. The different lithofacies characteristics of the oil content and its controlling factors were systematically evaluated, and an oil enrichment geological model of HSR was summarized. This research provides a geological basis for evaluating and building a reasonable interpretation model of HSR sweet spots.

2 GEOLOGICAL BACKGROUND

The HSR of the Middle Permian Lucaogou Formation was taken as study object, which located in the Jimusar Sag, east of the Junggar Basin (in **Figure 1**) (Xiao et al., 2021). The Jimusar sag is bounded by the Laozhuangwan fault, the Xidi fault, the Santai fault, and the Jimusar fault. The overall area is about 1270 km^2 (Yang et al., 2019), and it can be divided into the eastern slope area and the western sag area. The eastern slope is the main development area of unconventional oil reservoirs, and portions wells have obtained industrial oil flow (Pang et al., 2018). The western region has a low degree of exploration and is in the early stage of exploration but has enormous resource potential.

The Jingjingzigou Formation (P_2j), Lucaogou Formation (P_2l), and Wutonggou Formation (P_2wt) are found in the bottom, middle and top of Jimusar Sag, respectively. During the Lucaogou deposition period, lacustrine delta facies developed in the eastern slope area. And lacustrine sediments were primarily deposited in the western depression area. The thickness of the Lucaogou Formation ranges between 25 and 300 m, with an average thickness of up to 200 m. The burial depth gradually increases from east to the west, and the deepest part of Well JY-1 exceeds 4,800 m, with an average depth of 3,570 m. The deeper burial depths in the western sag will result in different temperature and pressure conditions in the same sag, which will affect key parameters for resource evaluation such as the lithology, physical properties, and oil-bearing properties. The Lucaogou Formation can be divided into two layers (P_2l_1 and P_2l_2), which are mainly composed of interbedded dolomite, sandstone, and mudstone. The source rock and reservoir of the Lucaogou Formation are frequently interbedded, and it is a typical HSR oil reservoir of source-reservoir interbeds and source storage adjacent (Huang et al., 2013).

3 MATERIALS AND METHODS

A total of 47 samples were collected from P_2l_1 in the western depression area of the Lucaogou Formation. Among them, 7 samples were from well JTX-B, 28 samples were from well JTX-A and 12 samples were from well JTX-X. The samples were retrieved following systematic sealed coring to ensure maximum preservation of the original fluid in the HSR. **Figure 2A** shows the location information of the sample. **Figure 2B** shows a schematic diagram of the sample processing. All samples were used to analyze lithology, physical properties, and oil content. Experimental data were obtained from the Jilin Oilfield Exploration and Development Research Institute.

3.1 Mercury Intrusion Capillary Pressure

MICP analysis of all HSR cores was carried out following the SY/T 5346-2005 standard. The analysis of the HSR samples was conducted at a temperature of 25°C, a humidity of 20% and at atmospheric pressure using an Autopore IV 9505 pore analyzer. The contact angle between mercury and the sample surface is 140°, the surface tension of mercury is 480 dyn/cm, and the pore size range is greater than 3.0 nm.

Previous studies have established many fractal dimension models based on high-pressure mercury injection curves. Although the fractal dimensions calculated by different models may be various, the complexity and heterogeneity of the pore structure in the representative reservoir rocks are similar. Because these models are all derived from a power function that describes the fractal characteristics of porous media (He and Hua 1998). MICP effectively describes the relationship between pore size and pore throat, which is a critical factor controlling reservoir permeability. Pores have self-similarity within a specific scale, and pores at different scales have different fractal dimensions. Therefore, fractal theory can be used to guide the division of different pore types. According to the Laplace-Washburn (1921) equation, the pore size distribution can be obtained from the mercury intake curve:

$$r = \frac{2\sigma \cos\theta}{P_C} \tag{1}$$

Where P_C is the mercury inlet pressure (MPa), r is the aperture (μm), σ is the surface tension (N/m), and θ is the contact angle (°).

The fractal characteristics of pores obtained in MICP analysis can be expressed by the following mathematical equation:

$$S_{Hg} = 1 - \left(\frac{P_C}{P_{C,\,min}}\right)^{D-3} \tag{2}$$

From **Eq. 2** we get:

$$\lg\left(1 - S_{Hg}\right) = (D-3)\lg p_c - (D-3)\lg p_{cmin} \tag{3}$$

Where P_C is the mercury inlet pressure (MPa), PC, min is the minimum capillary pressure, S_{Hg} is the cumulative mercury inlet percentage of the hole, and D is the fractal size of a dimensionless series.

3.2 Quantitative Grain Fluorescence on Extract

QGF-E analyses of all HSR cores were carried out following the SY/T 7309-2016 standard. The analyses of the HSR samples were conducted at a temperature of 24°C and a humidity of 20% using a Varian Cary-Eclipse particle luminometer under atmospheric pressure. The instrument specifications were: a flashing xenon lamp was used as the light source. The flashing half-peak width was approximately 2 μs. The peak power was equivalent to 75 Kw. The bandwidth was 1.5, 2.5, 10, and 20 nm. The scanning speed reached 24,000 nm/min. The excitation wavelength was 200–900 nm. The emission wavelength was 200–900 nm.

The QGF-E method is an economical and rapid technique used in the oil industry to detect oil content. The QGF-E spectrum represents the fluorescence characteristics of the adsorbed hydrocarbons on the surface of the reservoir particles, which can be used to determine the current oil layer or residual oil layer in exploration and drilling

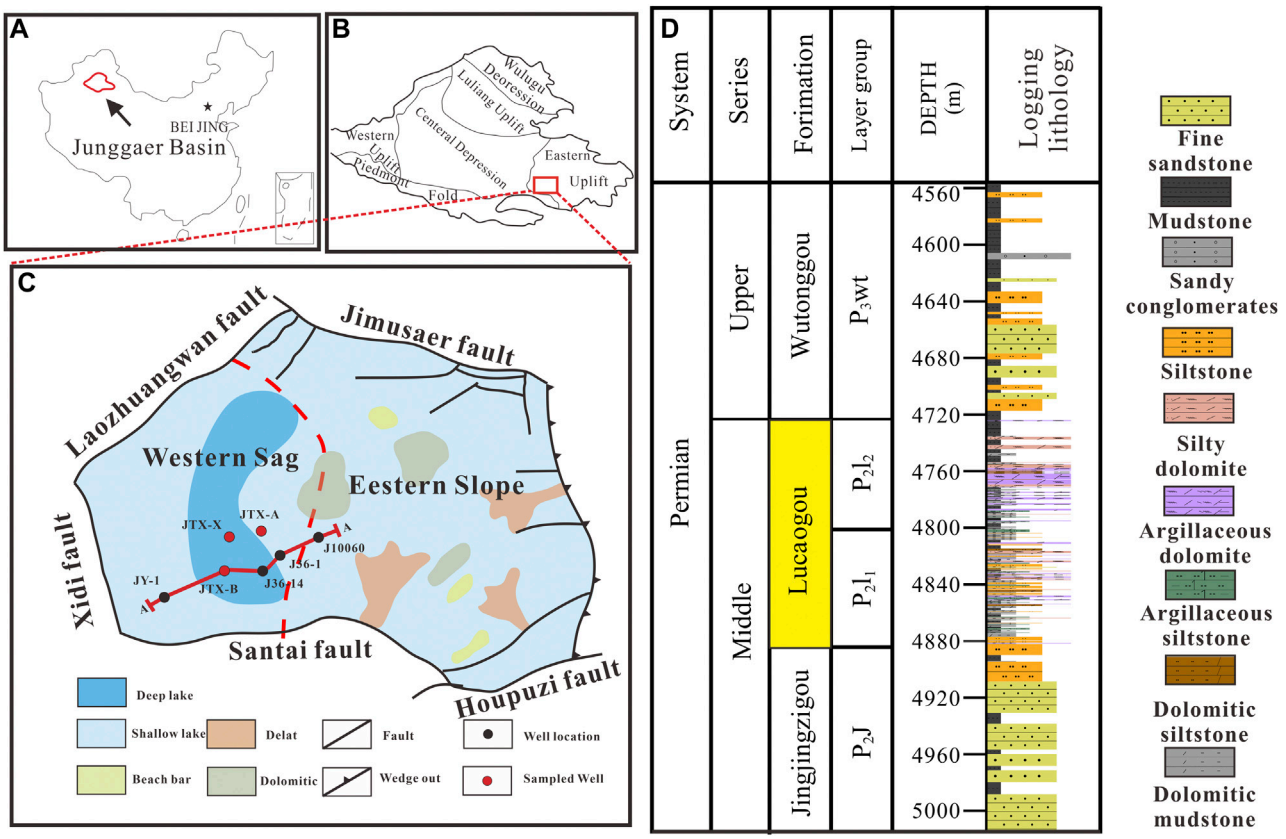

FIGURE 1 | (A) Location of Junggar basin; **(B)** Location of Jimusar depression; **(C)** Typical stratigraphic column of Jimusar depression; and **(D)** The general lithologic stratigraphy of Jimusar sag.

evaluation. Studies have shown that the QGF-E spectra of the current oil layer or residual oil layer samples have relatively high fluorescence intensities. The fluorescence peak width of heavy oil is approximately 475 nm, and the average value is between 475~600 nm. When the fluorescence spectrum intensity is between 375~475 nm, the QGF-E spectrum intensity of the water layer sample is very low, which is consistent with the fluorescence spectrum of dichloromethane solvent at 320–370 nm. Therefore, the strength of QGF-E can reflect the content of adsorbed hydrocarbons on the surface of reservoir particles, and the content of adsorbed hydrocarbons is positively correlated with oil saturation. The greater the strength of QGF-E is, the higher the oil saturation. The λ_{max} parameter reflects the composition and density of crude oil, while intensity represents oil saturation. When the strength of the QGF-E intensity is higher than 40 PC, there is a confident oil and gas exhibition in conventional sandstone reservoirs (Liu and Eadington 2005).

3.3 Two-Dimensional Nuclear Magnetic Resonance

2D-NMR analysis of all HSR cores was carried out following the SYT-6490-2007 standard. The analysis of the HSR samples was conducted at a temperature of 24°C, a humidity of 20% and at atmospheric pressure using an MR Cores-XX NMR unconventional core analyzer. The experimental frequency was 23 MHz with a 30 mm diameter probe, and the acquisition dead time was reduced to 15 μs so that the minimum T_2 response of solid organic matter in HSR could be measured.

The T_1-T_2 spectrum is a schematic diagram showing the distribution of different hydrogen atoms in the rock. Previous studies have shown that the T_1-T_2 spectrum can be divided into five signal areas, of which the approximate dividing line is called Zone 1 with $T_1 = 10$ ms, and is identified as the signal area of solid organic matter. Zone 2 is 0.2 m < T_2 < 1 ms and $T_1/T_2 < 100$, and zone 3 is $T_2 > 1$ ms and $T_1/T_2 > 10$. These latter two zones are considered to be the regions where oil is adsorbed and free oil is present. However, during the test, it was found that these two zones were difficult to distinguish. Zone 4, in the lower-left corner is a compound rich in hydroxyl groups, usually considered a hydroxyl group or a water-bound area, but kerogen may cause area 1 and Zone four to overlap. Finally, the lower right corner of the spectrum is Zone five, which usually signals the presence of free water in the pores or microcracks, but the adsorbed water on the surface of some clay minerals may also increase the signal in this area (Li et al., 2019).

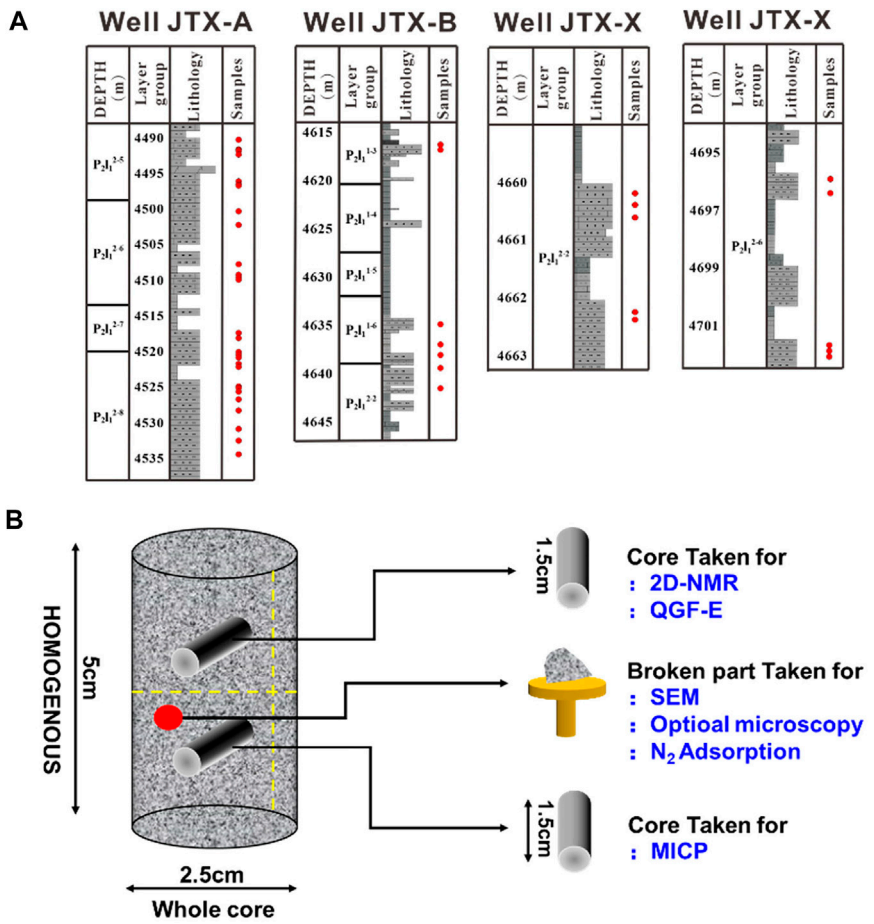

FIGURE 2 | (A) Sample location within each well; **(B)** Schematic diagram of sample processing.

3.4 Other Test Analyses

Low-temperature nitrogen adsorption/desorption analysis of all HSR cores was carried out following the ISO-9277/GB/T19587-2004 standard. The analysis of the HSR samples was conducted at a temperature of 25°C, a humidity of 30~46% and at atmospheric pressure using an American Mike ASAP2460 analyzer. Field emission scanning electron microscopy analysis of all HSR cores was carried out following the GB/T 18295-2001 standard. The analysis of the HSR samples was conducted at a temperature of 26°C, a humidity of 60% and at atmospheric pressure using a FEI Quanta 200F field emission scanning electron microscope. The magnification ranged from × 500 to × 20,000, which corresponds to resolutions of 500 to 12.5 nm.

4 RESULTS

4.1 Lithofacies Types

4.1.1 Mineral Composition and Lithology

The mineral composition of HSR within the Lucaogou is characterized by complexity and heterogeneity (**Figure 3**). Mineral is mainly composed of detrital (feldspar + quartz) and carbonate. P_2l_2 of the sag has a higher clay content than P_2l_1. This may be because P_2l_2 is the cover of the sag. In addition, the pyrite has developed in this area. Since pyrite has conductive properties, it may cause abnormal reservoir resistivity and lead to poor applicability of conventional logging (Xiao et al., 2021). These complex mineral combination characteristics are different from HSR in other basins. This reflect a kind of HSR in the transition between clastic sedimentary rock and chemical sedimentary rock (or the transition between volcaniclastic rock and normal sedimentary rock).

Based on systematic core observations, thin section analysis, and XRD analyses, the lithological characteristics of the western depression area of the Lucaogou Formation in Jimusar are revealed. The results further show that the Lucaogou Formation, which has a shallow lake sedimentary background, can be divided into two parts. The upper part represents a transgression, and the lower part represents the sediment from a regressive system (Qiu et al., 2016). The lithology mainly has the following characteristics in the Lucaogou. It is variable and changes quickly in the vertical direction, and is primarily partitioned in thin interbedded layers. There are various types of minerals, primarily transitional rocks consisting of clastic and chemical rocks. The lithology is divided into more than 20

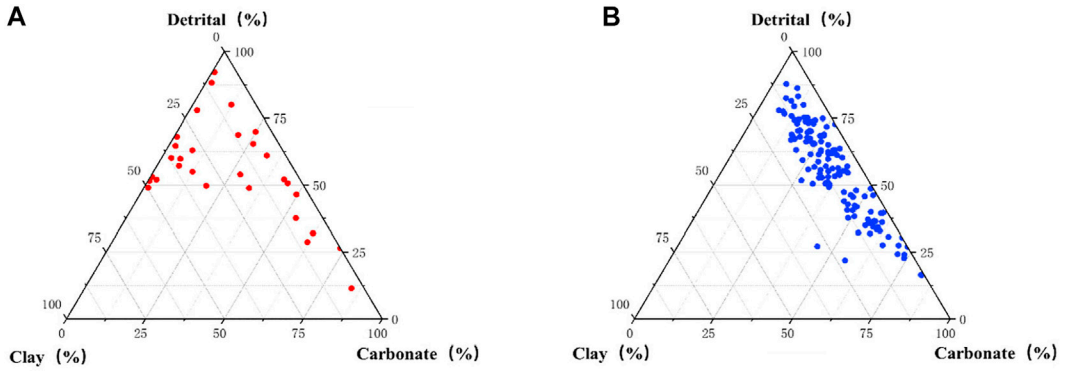

FIGURE 3 | Ternary diagrams of the mineral composition. **(A)** P_2l_2 mineral composition and; **(B)** P_2l_1 mineral composition.

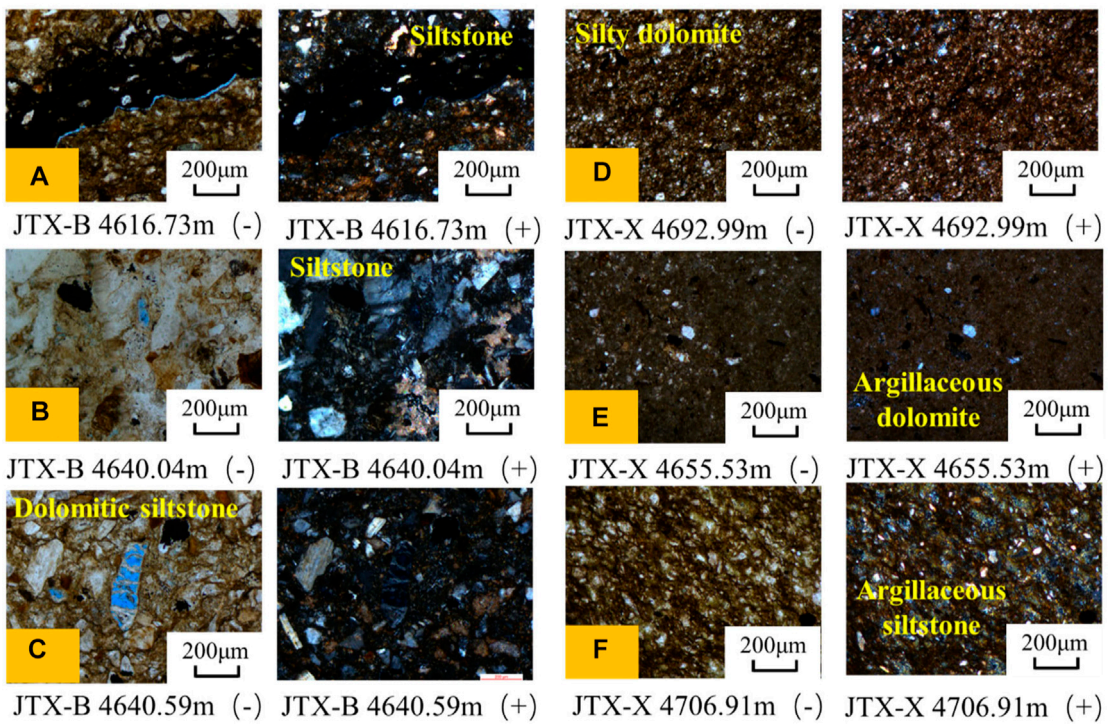

FIGURE 4 | Photomicrographs of reservoir rocks. **(A)** and **(B)** Siltstone; **(C)** Dolomite siltstone; **(D)** Silty dolomite; **(E)** Argillaceous dolomite; and **(F)** Argillaceous siltstone.

categories in the Lucaogou, including the following main lithologies: argillaceous dolomite, silty dolomite, siltstone, dolomitic siltstone, argillaceous siltstone, dolomitic mudstone, and mudstone.

Figure 4 shows that organic matter bands also exist in the siltstone, which may be due to the accumulation of multicomponent mixed sediments. Dolomite siltstone has dissolved pores and shows an uneven suture structure. Silty dolomite exhibits terrigenous clasts and a large amount of organic matter, a small amount of carbon chips, and pyrite, and the rock is relatively dense. Argillaceous dolomite contains terrigenous clastic, a small amount of asphalt and carbonaceous rocks which are relatively dense, and no pores are observed; argillaceous siltstone is dense with poor physical properties.

4.1.2 Lithofacies

Lithofacies can reflect the accumulation, depositional process, and chemical characteristics (He et al., 2018) of organic matter, and it is a complete manifestation of all essential characteristics of

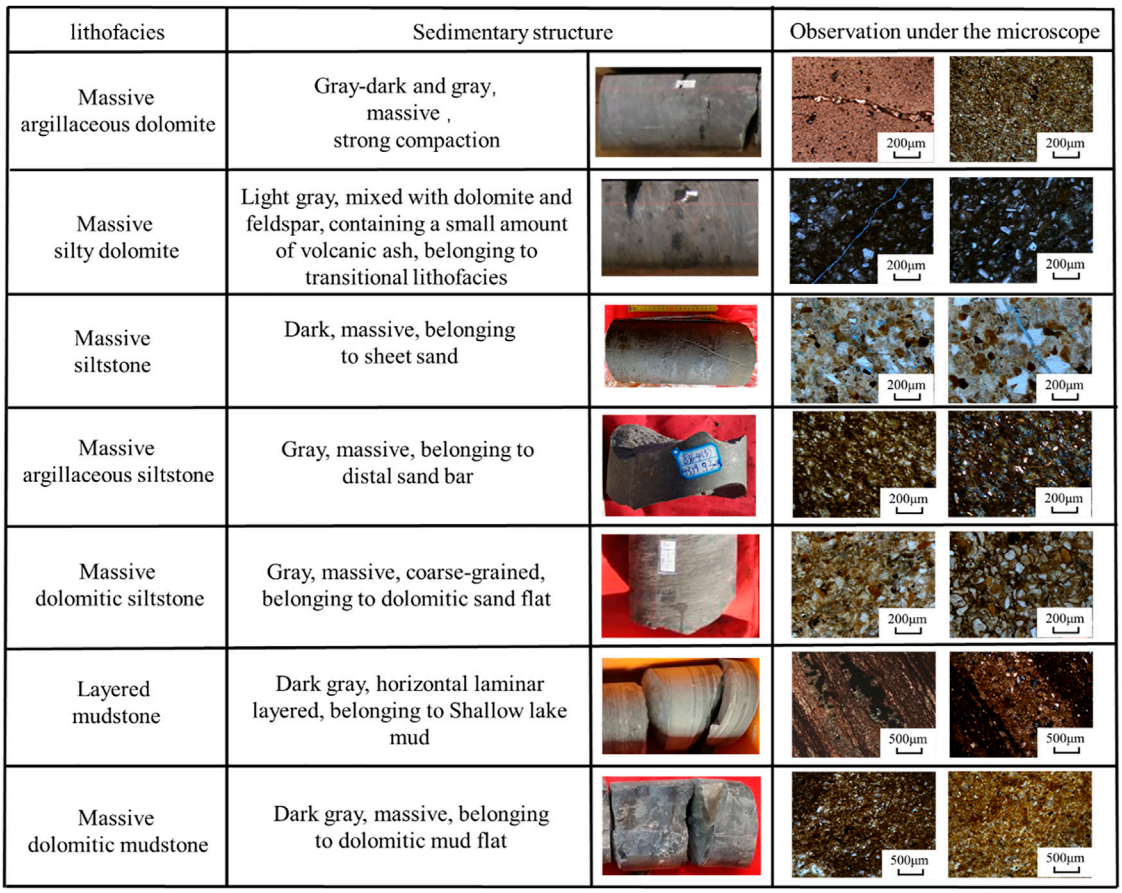

FIGURE 5 | Comparison of lithofacies type.

rocks (He et al., 2022). In addition, lithofacies are also the basic unit of HSR reservoirs, which can be used to identify dominant reservoirs. The studies on HSR mainly consist of shale and carbonate rocks. Lithofacies classification of shale is mainly based on the characteristics of mineral composition, structure, biology, and bedding structure (Slatt and Rodriguez 2012). Previous scholars integrated the material composition, sedimentary structure, organic matter characteristics, and other factors such as bioturbation to divide the HSR facies types of the continental lake basin of the Lucaogou Formation in the eastern oblique section of the Jimusar into 26 types (Lin et al., 2021). We found that the HSR reservoirs of the Lucaogou Formation in western Jimusar mainly contain seven lithofacies (**Figure 5**), including massive argillaceous dolomite lithofacies, massive silty dolomite lithofacies, massive siltstone lithofacies, massive argillaceous siltstone lithofacies, massive dolomitic siltstone lithofacies, layered mudstone lithofacies, and massive dolomitic mudstone lithofacies.

Figure 5 shows that massive siltstone lithofacies and massive dolomitic siltstone lithofacies may be the main dominant reservoirs. The cores from these lithofacies are generally gray-black, with thin sections showing grains, microcracks and pores, and the oil-bearing grade are oil trace and oil immersion. Massive argillaceous siltstone lithofacies are generally gray, with thin sections showing fine-grained features and they belong to distal sand bar microfacies. Massive silty dolomite lithofacies are coarser than the massive argillaceous dolomite lithofacies, and both cores are gray, but the former has cracks. Layered mudstone lithofacies are generally black-gray, with obvious bedding and compact rocks. Massive dolomitic mudstone lithofacies cores are generally black–gray, with undeveloped bedding and dense rocks.

4.1.3 Spatial Distribution of Lithofacies

The HSR reservoir is effectively-identified based on conventional logging data combined with nuclear magnetic logging data and lithology scanning logging data. However, due to frequent interbedded strata, to better reveal the law of lithofacies change of HSR, five types of lithofacies combination of HSR were summarized, according to the lithofacies change characteristics and sedimentary sequence.

Single dolomite lithofacies (**Figure 6A**) refers to a set of strata dominated by dolomite (greater than 50%). The lithofacies is dominated by argillaceous dolomite, with a small amount of silty dolomite and dolomitic siltstone. This lithology type is mainly formed in the coastal dolomitic flat sedimentary environment.

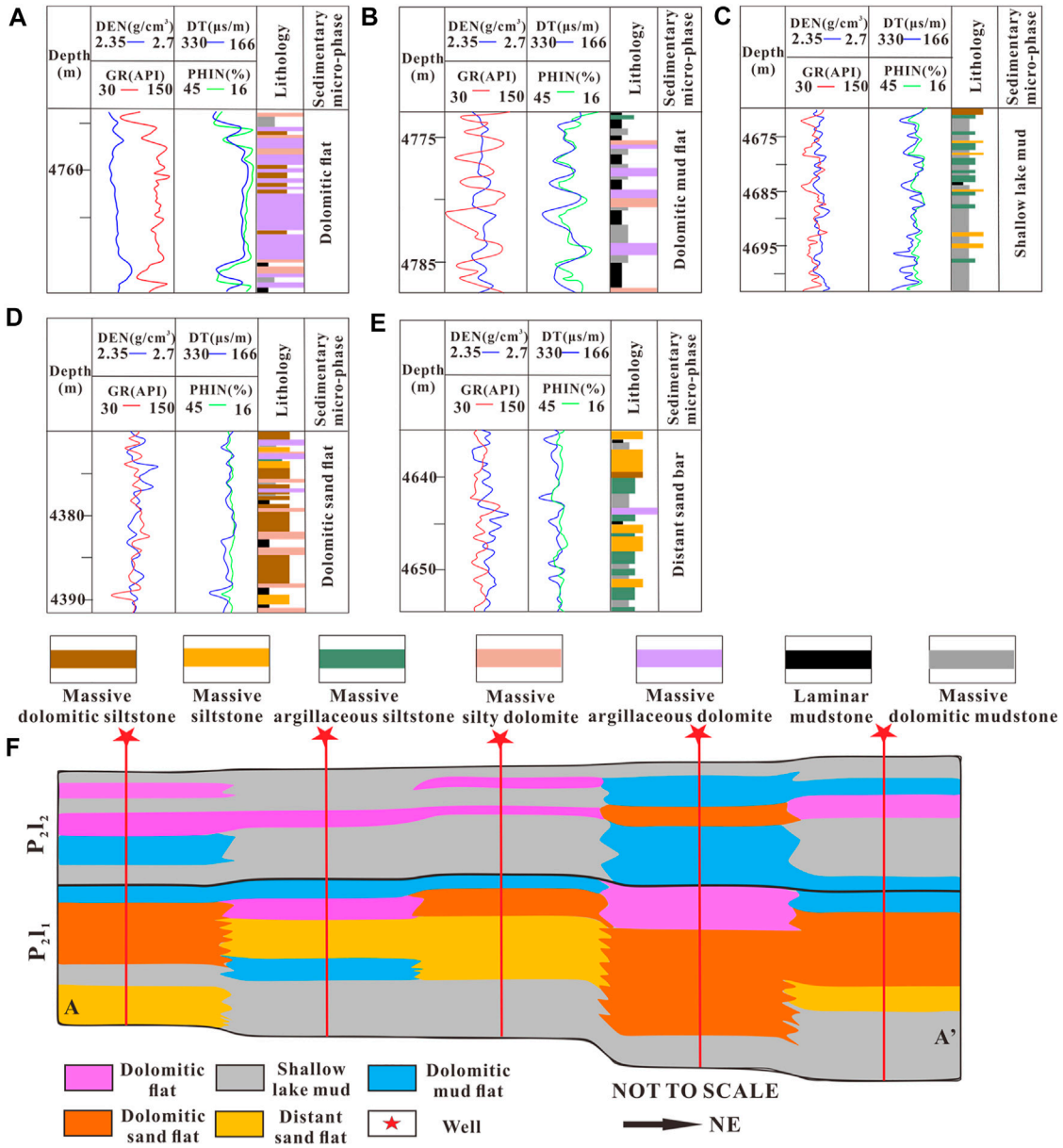

FIGURE 6 | Lithofacies assemblage type of the Lucaogou Formation. **(A)** Single dolomite lithofacies; **(B)** Interlayered dolomitic mudstone and dolomite lithofacies; **(C)** Inter-layered argillaceous siltstone and dolomitic mudstone lithofacies; **(D)** Dolomitic siltstone and argillaceous sandstone facies; **(E)** Argillaceous siltstone and siltstone lithofacies; and **(F)** Northeast-Southwest cross section of the Lucaogou Formation in the Jimusar Sag, Junggar Basin, showing the correlation between the different lithofacies and sedimentary environment.

The hydrodynamic force is weak, and the salinity of the water is high, which is conducive to the precipitation of carbonate minerals. When the hydrodynamic force becomes stronger, it will increase the terrestrial input and develop a dolomite siltstone or silt sandy dolomite interlayer.

Interlayered dolomitic mudstone and dolomite lithofacies is shown in **Figure 6B**. This type of lithofacies is mainly formed in a dolomitic mud flat sedimentary environment. The lithofacies is dominated by dolomitic mudstone interbedded with dolomite, of which mudstone accounts for more than 50%. This type of assemblage is formed in a relatively deep-water environment, and the salinity of the water is lower, which is not favorable to the formation of dolomite. As the water becomes shallower, if evaporates and the salinity becomes higher, allowing carbonate rocks to locally develop. This type of lithofacies combination makes it difficult to form an effective reservoir.

Interlayered argillaceous siltstone and dolomitic mudstone lithofacies are shown in **Figure 6C**. The lithofacies is dominated by dolomitic mudstone, with thin layers of siltstone and argillaceous siltstone. Dolomite is underdeveloped, and the

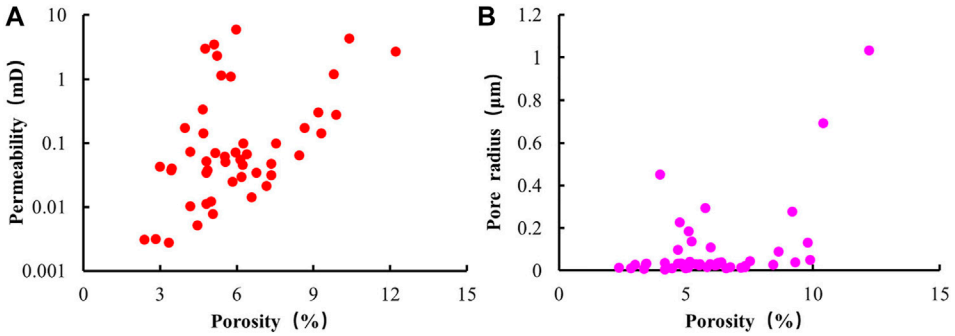

FIGURE 7 | (A) The relationship between porosity and permeability; **(B)** The relationship between porosity and pore size.

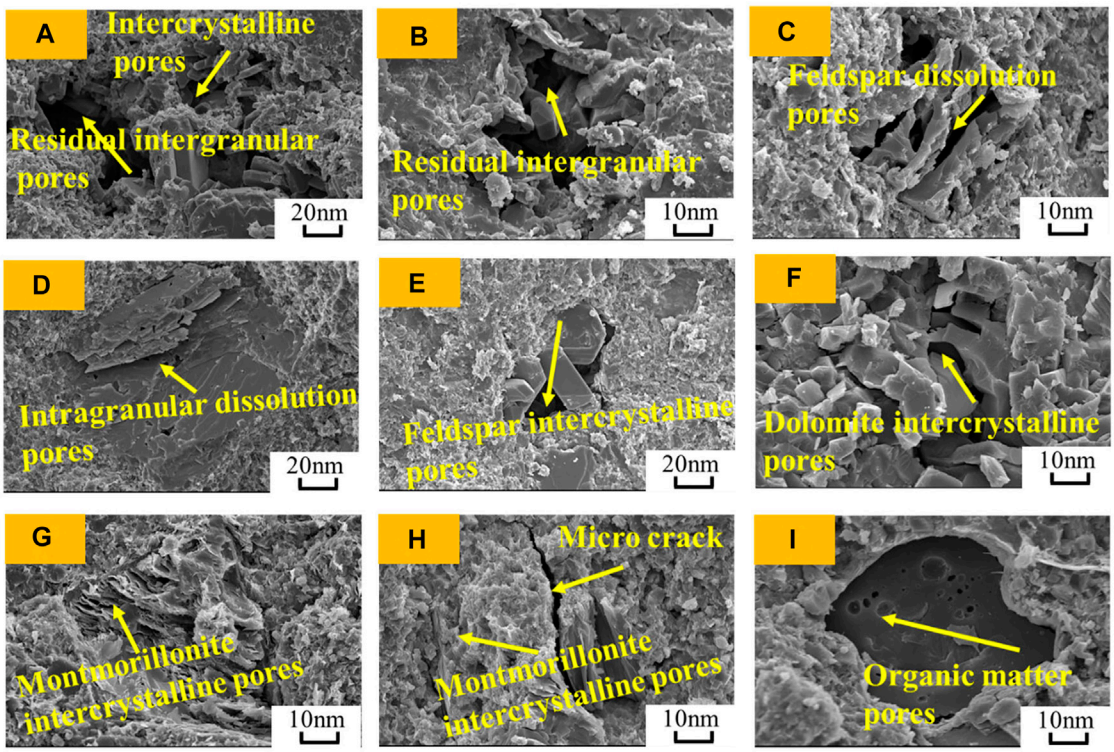

FIGURE 8 | SEM Pore Type Diagram. **(A)** Inter-crystalline pore and residual intergranular pore; **(B)** residual intergranular pore; **(C)** Feldspar dissolution pores; **(D)** Intragranular dissolution pores; **(E)** Feldspar intergranular pore; **(F)** Dolomite inter-crystalline pores; **(G)** Montmorillonite inter-crystalline pores; **(H)** Microcrack and montmorillonite inter-crystalline pores; and **(I)** organic matter pores.

thickness of the mudstone is >50%. This type of lithology is mainly formed in a shallow lake mud sedimentary environment. Similar to the interlayered dolomite mudstone and dolomite lithofacies, it also formed in a deeper water environment, but it was more affected by the source input. Due to the transformation and transportation of lake waves, thin layers of siltstone or argillaceous siltstone can also be formed in a deep-water environment (Kuang et al., 2012). Good reservoirs can be formed in localized areas.

Dolomitic siltstone and argillaceous sandstone lithofacies are shown in **Figure 6D**. Dolomitic siltstone is dominant, and interbedded with silty dolomite and argillaceous siltstone, of which dolomite siltstone accounts for more than 50%. This type of assemblage is mainly formed in the sedimentary environment of the dolomitic sand flat (Zhang et al., 2017). The water has high salinity, the lake wave reformation effect is strong, and the provenance influence is prevalent. Under the dual action of land-source mechanical transportation and chemical

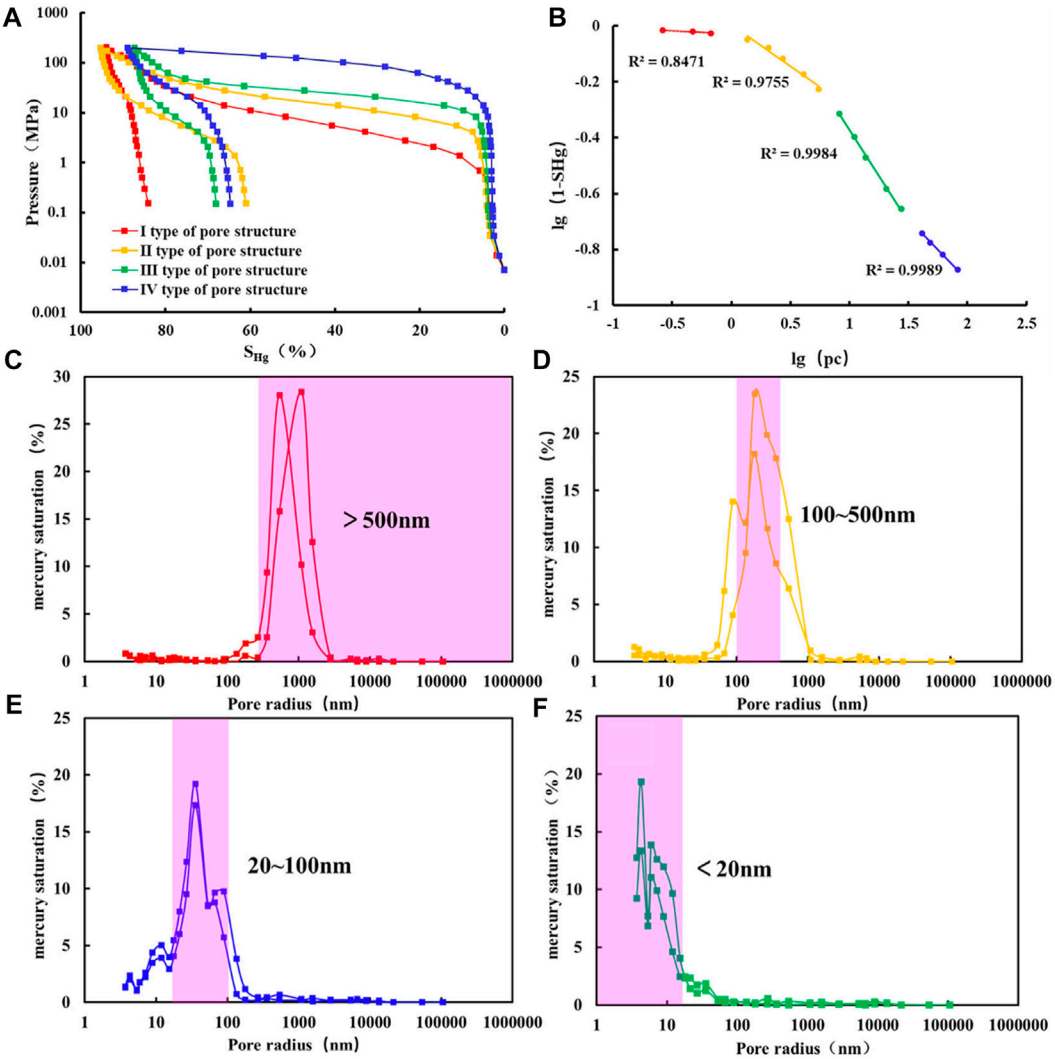

FIGURE 9 | (A) Typical MICP features; **(B)** Typical MICP fractal features; and **(C–F)** MICP pore size distribution characteristics.

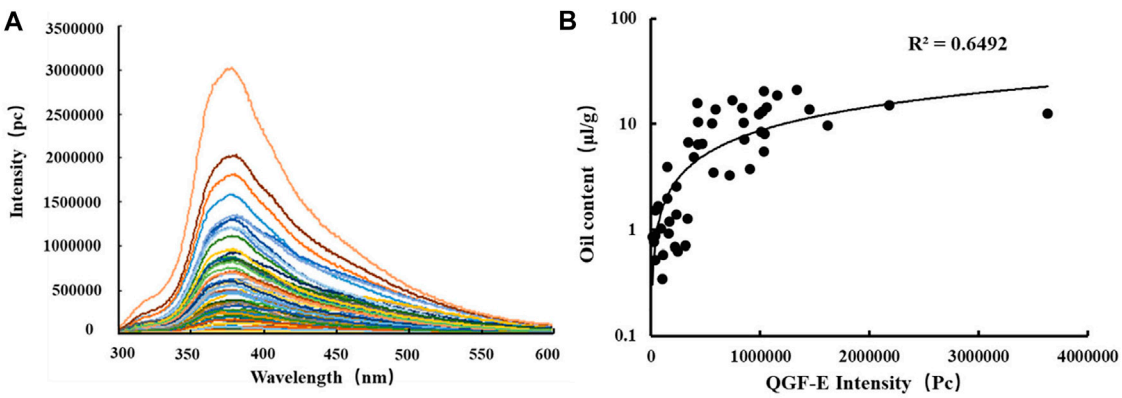

FIGURE 10 | (A) QGF-E analysis; **(B)** Relationship between oil content and QGF-E intensity.

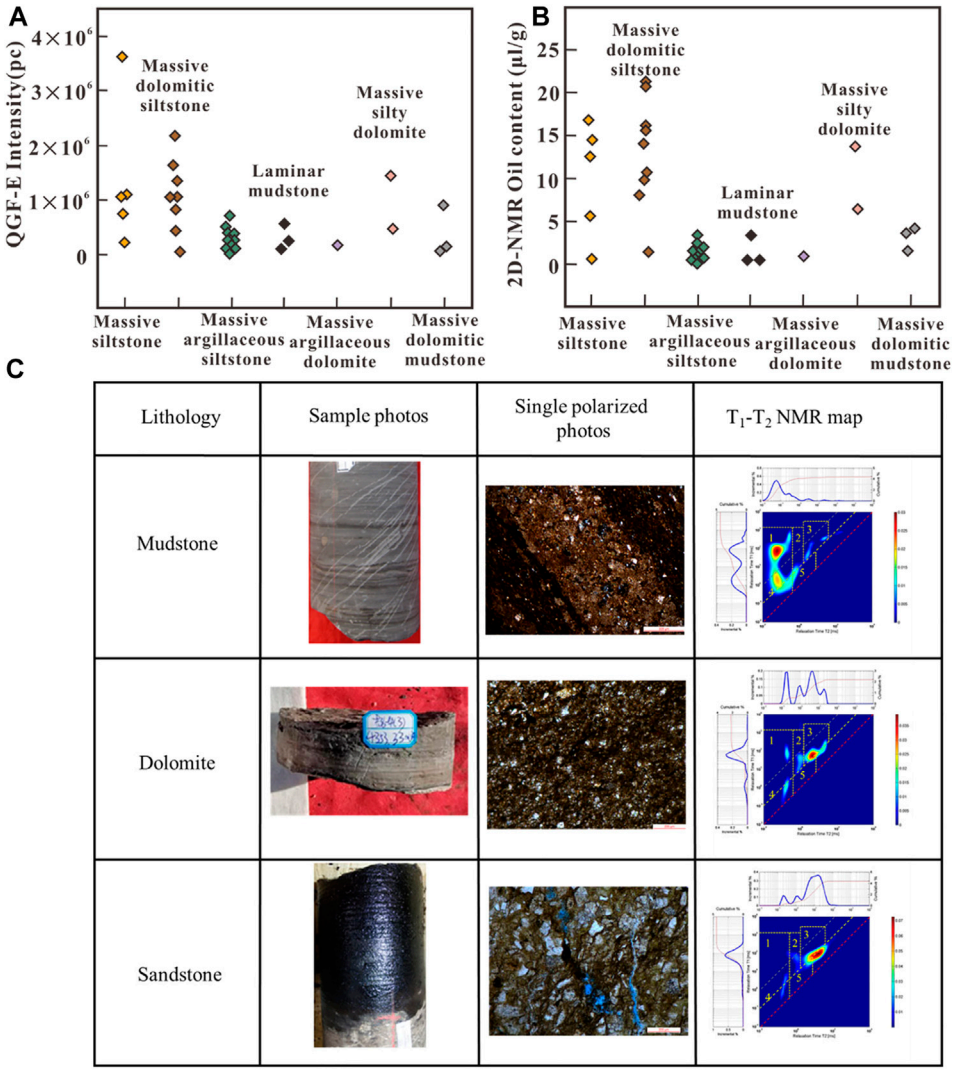

FIGURE 11 | Oil content analysis of different lithofacies. **(A)** The relationship between lithofacies and QGF-E intensity. **(B)** The relationship between lithofacies and 2D-NMR oil content. **(C)** The relationship between lithofacies and 2D NMR map.

deposition, a large area of clastic-sand flat deposits is formed. This type of combined reservoir is relatively developed and is the main lithofacies involved in oil enrichment.

Argillaceous siltstone and siltstone lithofacies (**Figure 6E**), are mainly composed of siltstone and argillaceous siltstone, with thin layers of argillaceous dolomite and dolomitic siltstone, of which dolomite is <20% and siltstone is >30%. This type of assemblage is formed in the distal sand bar or sheet sand deposits of a delta front, near provenance and with strong wave transformation, which is not conducive to carbonate sedimentation, and the dolomitic content in the rock is low. This type of combined reservoir is also conducive to oil accumulation (Zhang et al., 2019).

Figure 6F shows the lithofacies assemblage cross-section. The result shows that the lithofacies distribution presents the shape of a "sandwich." The lower and upper parts are mainly composed of interlayered dolomitic mudstone and dolomite lithofacies and interlayered argillaceous siltstone + dolomitic mudstone lithofacies (dolomitic mud flat and shallow lake mud sedimentary environment). The middle is mainly dolomitic siltstone, argillaceous sandstone lithofacies, argillaceous siltstone and siltstone lithofacies (dolomitic sad flat and distal sand bar sedimentary environment). In addition, whole dolomite is mixed with single dolomite lithofacies (dolomitic flat sedimentary environment).

It can be seen from stratigraphic section A to A' in **Figure 6F**, and the position of the stratigraphic section is shown in **Figure 1**. The stratigraphic section shows the depth of the water changing from deep, to shallow, to deep again. The dolomitic mudstone and dolomite interlayer lithofacies developed on the top of P_2l_2 and the bottom of P_2l_1 is

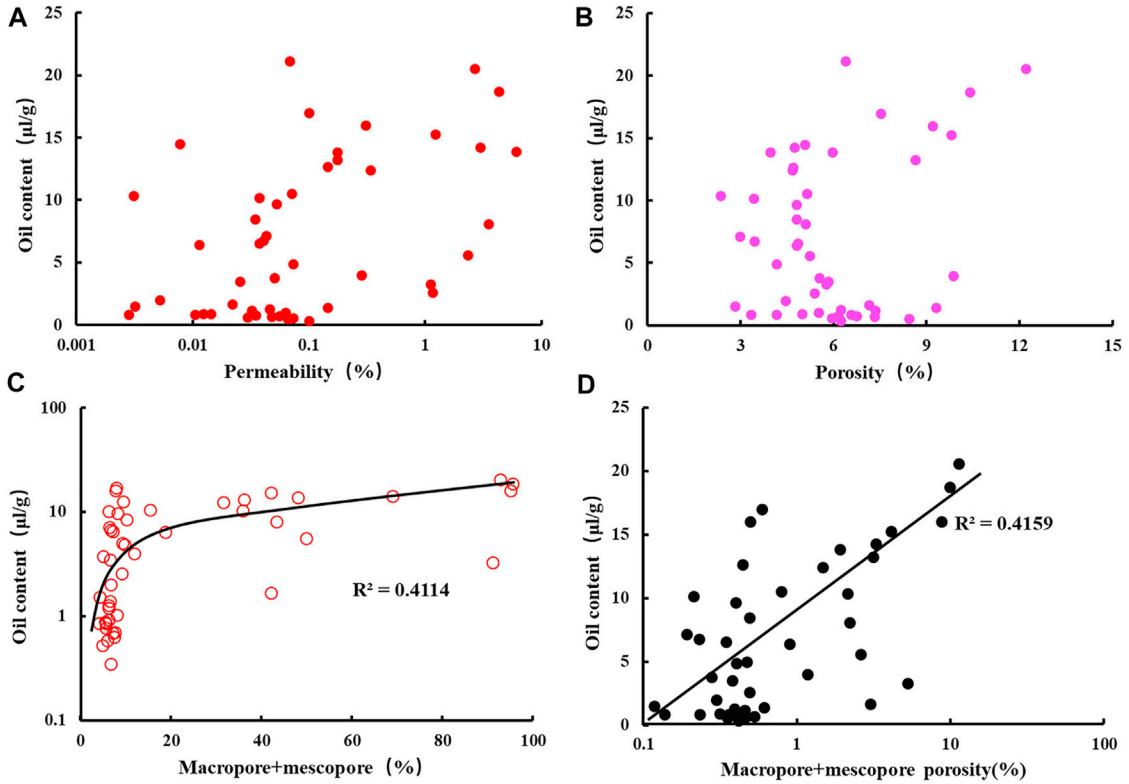

FIGURE 12 | (A) The relationship between permeability and oil content; **(B)** The relationship between porosity and oil content; **(C)** The relationship between macropore + mesopore proportion and oil content; and **(D)** The relationship between macropore + mesopore porosity and oil content.

remains in the sedimentary areas of the shallow lake mud and dolomitic mud flat. It is continuous and thick, and can be used as a roof and floor for capping, thereby effectively preventing the oil generated from the source rock from migrating outwards. The oil generated in the shallow lake mud and dolomitic mud flat sedimentary area can migrate to the dolomitic sand flat and distal sand bar sedimentary areas in the central part, and accumulate to form an oil reservoir close to the source and reservoir. Because of the existence of shallow lake mud and dolomitic mud flat sedimentary areas, siltstone, dolomite, and source rock frequently interbed, and the oil generated from the source rock can also be stored in it, forming a source-reservoir integrated oil reservoir. Among them, the exploration and development prospects of the source-reservoir adjacent oil reservoir may be greater than that of the source-reservoir integrated type.

4.2 Physical Characteristics

Figure 7 shows the basic physical characteristics of the Lucaogou Formation. The results show that the porosity of samples in the western Lucaogou Formation range from 2.36 to 12.21%, and the average porosity is 5.94%. The permeability range is 0.003–6.043 mD, and the average permeability is 0.58 mD. According to the MICP, the pore radius of the core samples range from 0.008 to 1.035 μm, with an average value of 0.098 μm. Overall, the relationship between porosity and permeability is complicated, and there is a poor relationship between porosity and pore radius, mainly due to low porosity and ultralow permeability with typical compact characteristics.

4.2.1 Pore Type

Figure 8 shows a SEM pore type diagram. The results show that HSR develops storage spaces of different scales. According to the genesis of pores, the types of storage spaces are divided into two categories: primary pores and secondary pores. Furthermore, they can be subdivided into five types: residual intergranular pores, intergranular dissolved pores, intragranular dissolved pores, intercrystalline pores, and organic pores. At the same time, there are also local microcracks.

The shape of the residual intergranular pores (**Figures 8A,B**) is mainly elongated, and irregular polygons. The pores remaining mainly after the primary intergranular pores are compacted and cemented, and most of them appear around brittle minerals such as feldspar particles and quartz particles. The pore diameter is usually less than 50 μm, and such pores are mainly developed in the coarse-grained facies.

The shapes of the dissolution pores (**Figures 8C,D**) are mainly long-narrow and jagged, mainly due to pores formed by the dissolution of minerals such as feldspar and dolomite by an acidic liquid. The intergranular dissolution pores have good connectivity, which can significantly improve the physical properties of the reservoir. However, most of the intragranular

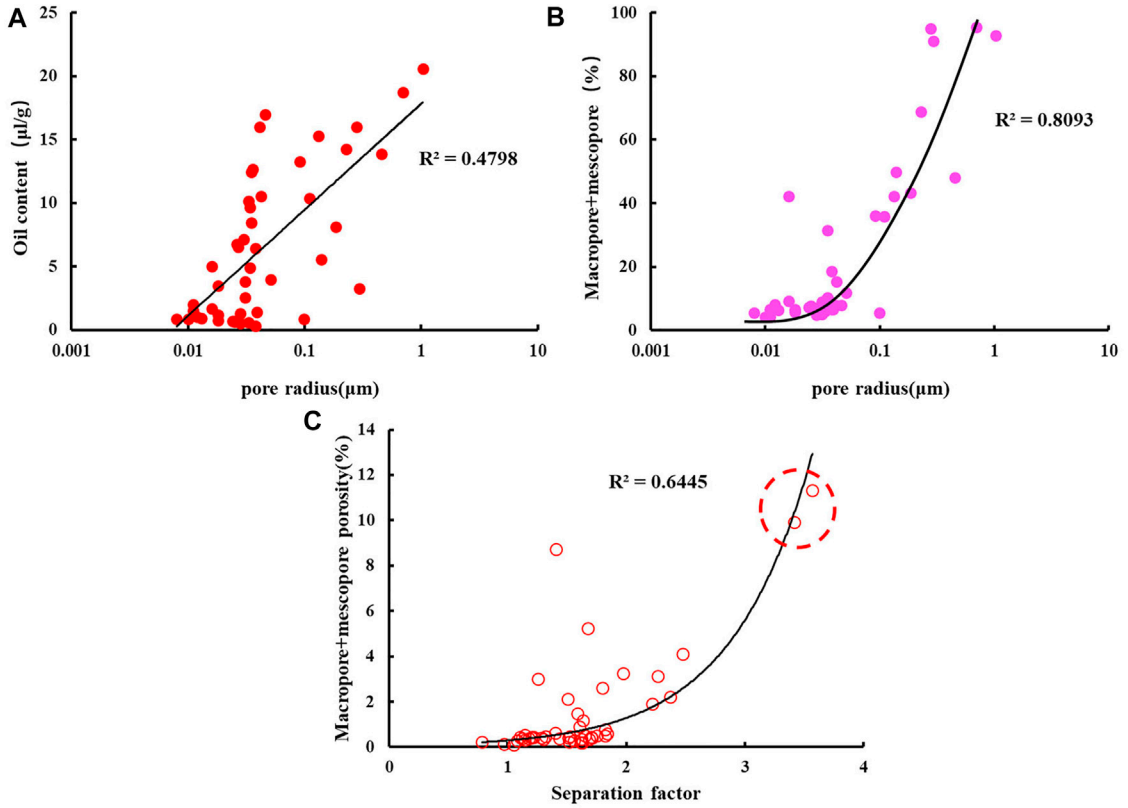

FIGURE 13 | The relationship between pore structure and oil content. **(A)** The relationship between pore radius and oil content. **(B)** The relationship between pore radius and the proportion of macropore and mescropore. **(C)** The relationship between pore radius and macropore and mescropore porosity.

dissolved pores have poor connectivity, and whether they improve the reservoir's physical properties is not apparent.

The shapes of the inter-crystalline pores (**Figures 8E–H**) are mainly regular polygons and flakes, mainly formed by the growth of mineral crystals such as dolomite, feldspar, quartz, and clay. Microfractures (**Figure 8H**) are mainly caused by compaction and tectonic stress, which significantly affect the physical properties of the reservoir and are relatively less developed in the area.

Organic pores (**Figure 8I**) are mostly elongated and elliptical, their pore diameters are generally small, and the improvement effect of organic pores on the reservoir's physical properties is not obvious.

4.2.2 Pore Structure Characteristics

MICP can reveal the pore throat size, connectivity, and sorting information of rocks by recording the process of mercury introduction and mercury withdrawal. The pore throat structure of the HSR reservoir is extremely heterogeneous. The maximum mercury saturation range of the samples is 31.65–97.39%, and the average is 84.98%. The range of the median pore throat radius is 0.006–0.927 μm, and the average is 0.072 μm. The sorting coefficient is between 0.784~3.567, and the average is 1.605.

According to previous studies, pores have self-similarity within a specific scale. (Li et al., 2013). Therefore, fractal theory and cluster analysis can be used to classify pore structure types. Observing the MICP of 47 samples, mercury inflection points generally exist near the three mercury intrusion pressure points of 0.67, 8.25, and 41.33 Mpa (**Figure 9A**). According to the Laplace-Washburn equation, the pore radii corresponding to these three inflection points are 500, 100, and 20 nm. According to fractal theory, these inflection points can be used as the boundaries for pore partitions.

Figure 9B shows that in the lg(1-SHg)-lgpc double logarithmic coordinate system, the mercury intrusion curve of the sample presents a segmented straight line, indicating that the reservoir pore space has multifractal characteristics. The point of intersection of the fractal and the three inflection points of the mercury intrusion curve are consistent with the mercury inlet pressure values. **Figure 9B** also shows that it is reasonable to divide the shale pore space into four intervals using the three inflection points obtained by the MICP injection curve. Macropores (pore radius >500 nm, **Figure 9C**) mainly correspond to pore types such as intergranular pores and intergranular dissolution pores. Mesopores (pore radius 100–500 nm, **Figure 9D**) correspond to intergranular dissolution pores and intragranular dissolution pores, and small pores (pore radius 20–100 nm, **Figure 9E**) mainly correspond to intragranular dissolution pores and inter-crystalline pores.

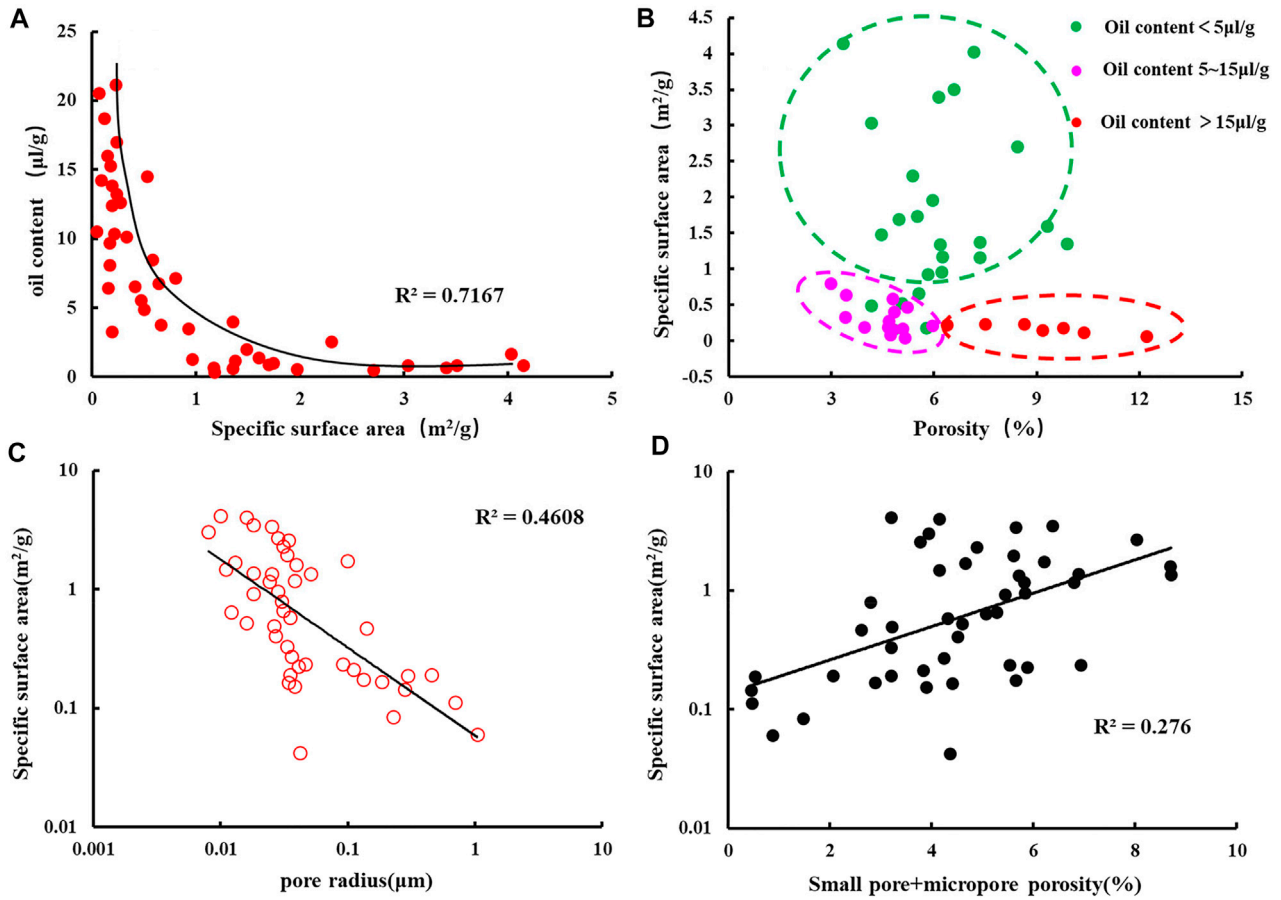

FIGURE 14 | (A) The relationship between specific surface area and oil content; **(B)** The relationship between porosity and specific surface area; **(C)** The relationship between pore radius and specific surface area; and **(D)** The relationship between samll pore + micropore porosity and specific surface area.

And micropores (pore radius <20 nm, **Figure 9F**) mainly correspond to clay inter-crystalline pores.

4.3 Oil Content

In the QGF-E experiment (**Figure 10A**), after normalizing the sample to 1 g of reservoir particles and 20 ml extraction solution, the fluorescence intensity ranged from at 11,329.2–3,631,111.2 PC, which is significantly higher than the QGF-E intensity of conventional sandstone reservoirs (Downare and Mullins 1995). The result shows a good hydrocarbon-bearing properties. Among them, λmax is between 367–411 nm, showing the characteristics of medium-light oil and a high content of medium components, and the heterogeneity of the oil content is substantial from a longitudinal point of view. 2D-NMR detection also obtained fluid data from the different rock samples. The total fluid volume was 141.81–897.23 μl, with an average of 405.16 μl. The content of hydroxyl group or bound water was 0–14.568 μl/g, with an average value of 3.599 μl/g. The free water content in pores or cracks was 0–3.343 μl/g, with an average value of 0.727 μl/g. The oil content was 0.35–21.162 μl/g, and the concentration was 7.292 μl/g. Among them, the oil content obtained by 2D-NMR has an apparent positive correlation with the strength of QGF-E (**Figure 10B**), which again confirms its excellent oil content.

5 DISCUSSION

5.1 Relationship Lithofacies and Oil Content

Figures 11A,B is the relationship between lithofacies and oil content. The results show that massive siltstone, massive dolomitic siltstone, and massive silty dolomite have higher oil content. Although the massive argillaceous sandstone facies have a relatively coarse grain size, its oil content is relatively low, due to cementation by minerals. Similar to conventional reservoirs, cementation can also damage HSR reservoirs. By observing the thin section, the most of the cementation occurs around the clastic particles, and blocks the intergranular pores. This resulted in the deterioration of the oil content of the massive argillaceous siltstone facies.

The rocks in the sweet spots correspond to massive dolomitic sandstone facies, massive siltstone facies, and massive dolomitic

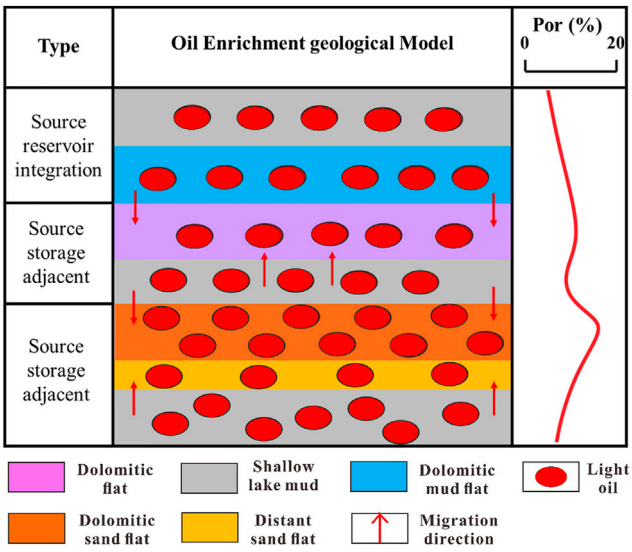

FIGURE 15 | Oil enrichment geological model of the Lucaogou Formation, Western Jimusar sag.

sandstone facies. High-quality source rocks should be layered mudstone facies and massive dolomitic mudstone facies. However, we combined thin sections (**Figure 4A**) and 2D-NMR (**Figure 11C**) to find organic matter in the sandstone facies and dolomite facies, which may be caused by mixed accumulation. Therefore, in addition to mudstone facies, other lithofacies can also have a particular hydrocarbon generation potential. This is one of the most distinct characteristics of HSR.

The mudstone T_1-T_2 map in **Figure 11C** shows a large amount of organic matter and a small amount of oil content in the region 1 and 3, the mudstone facies may be a source-reservoir integrated reservoir. When there is no migration channel around the mudstone facies, the mudstone facies themselves have a small number of pores and can store a certain amount of oil, but the oil content is minimal. The dolomite facies is a transitional facies with moderate physical properties but high oil content in T_1-T_2 map. This may be related to the oil-wetting characteristics of dolomite. Dolomite is oil-wet. Oil is easy to charge when dolomite dominates. Sandstone facies (except for massive argillaceous siltstone) is the best reservoir lithology in this area, with good physical properties and good oil-bearing properties. In addition, it also shows that oil is generated in mudstone facies and migrates a short distance to coarse-grained sandstone facies or to transitional dolomite facies to stay in rich integrated oil reservoirs.

5.2 Influence of Pore Structure on Oil Content

Figures 12A,B is the effect of porosity and permeability on the oil content of the reservoir. The results show that a positive correlation between permeability and oil content is not apparent. The relationship between porosity and oil content is very complicated and contradictory. Previous studies have shown that porosity is generally positively correlated with oil content (Lu et al., 2012; Li et al., 2015; Hu et al., 2018; Pang et al., 2018). However, other studies have shown that there are two contradictions between large porosity and low oil content and between minor porosity and high oil content (Cao et al., 2017) (**Figure 12B**).

According to the MICP fractal results, the more macropores and mesopores there were, the better the oil content properties of the reservoir. The reason may be related to the difference in wettability of different pore sizes. Previous studies have shown that the Lucaogou Formation HSR reservoir has higher oil saturation. Reservoir wettability is primarily neutral, followed by localized oil-wet (Xu et al., 2019). The surface of the larger pore throats are usually covered by an oil film, which have prominent oil wetting properties. While the relatively small pore throats have no oil film development. This means that macropores are lipophilic and oil-containing, while small pores are hydrophilic and water-containing (Wang et al., 2019; Xu et al., 2019). Therefore, the more macropores and mesopores there are (**Figures 12C,D**), the higher the oil content.

The micropore structure also has an effect on the oil content. Among them, the larger the pore radius is, the higher the oil content (**Figure 13A**). This is because the larger the pore radius is, the weaker the heterogeneity of pores and pore throats, which is more conducive to oil filling (**Figure 13B**). The heterogeneity of the pore structures can be expressed by the sorting coefficient. When the number of medium and large pores increases, the oil content increases linearly (**Figure 13C**). The separation factor is greater than 3 caused by micro-cracks.

5.3 Specific Surface Area Controls The Oil Content

The specific surface area controls the oil content. **Figure 14A** shows that the smaller the specific surface area is, the greater the oil content. **Figure 14B** shows that when the specific surface area is small enough ($A < 1\ m^2/g$), the oil content of the sample is positively correlated with the porosity. When the specific surface area of the sample is $> 1\ m^2/g$, the oil content is not related to the porosity. That is, no matter how large the porosity is, the oil content still low.

The specific surface area may affect oil content through pore radius. Pore radius is negatively related to specific surface area (**Figure 14C**). Furthermore, as the specific surface area increases, the number of micropores and small pores increases (**Figure 14D**), and oil filling becomes difficult. Therefore, when the surface area is large, the oil content is low. In this area, the macropores are highly oil-wet and the small pores are highly water-wet. When the proportion of micropores increases, the water-wet of the pore throats will increase, resulting in a decrease in oil content.

We have observed that some samples have large porosity and specific surface area. The proportion of small pores and micropores will increase when the specific surface area

becomes larger. This means that the macroporosity is formed by the accumulation of small pores and micropores. The oil content is not determined only by a single macroscopic physical property, but also by microscopic information such as the abundance of mesopores and macropores, specific surface area comprehensive evaluation.

5.4 An Oil Enrichment Geological Model

In general, the study area has the characteristics of overall oil content. We combined 2D-NMR and QGF-E experimental data to summarize two oil enrichment geological models of the Lucaogou Formation, Western Jimusar sag, Junggar Basin. One of the first, the oil generated in the shallow lake mud and dolomitic mud flat sedimentary areas can be micromigrated to the dolomitic sad flat and distant sand bar sedimentary areas. After accumulation, it is conducive to the formation of "source storage adjacent to the oil reservoirs."

The second of them, when the shallow lake mud and dolomitic mud flat sedimentary areas do not have a migration channel to the dolomitic sad flat and distant sand bar sedimentary areas, the oil generated in the shallow lake mud and dolomitic mud flat sedimentary areas can be accumulated to form a "source reservoir integrated" unconventional oil reservoir (**Figure 15**).

6 CONCLUSION

1) According to the material composition, sedimentary structure, and organic matter characteristics, the HSR in the western depression of the Lucaogou Formation in the Jimusar Sag is divided into seven categories: layered mudstone lithofacies, massive dolomitic mudstone lithofacies, massive argillaceous dolomite lithofacies, massive silty dolomite lithofacies, massive siltstone lithofacies, massive argillaceous siltstone lithofacies and massive dolomitic siltstone lithofacies.
2) Different lithofacies types have clear differences in their reservoir physical properties and oil content. In addition to the lithofacies and pore structure, the oil content is also controlled by the specific surface area. The oil content of the samples is very low, when the specific surface area exceeds 2 m^2/g.
3) Layered mudstone and massive dolomitic mudstone lithofacies have the worst physical properties and oil content properties. However, they do have high organic matter contents and are the main source rocks of the Lucaogou Formation. The massive argillaceous siltstone and massive dolomite lithofacies interbed frequently. Although their physical properties are moderate, oil reservoirs can be formed, due to the adjacent to the source rock. Massive dolomitic siltstone, massive siltstone, and silty dolomite lithofacies have the best physical properties and oil-bearing properties, with the highest proportion of mesopores and macropores. They are the best reservoirs in the Lucaogou Formation.
4) Two types of unconventional oil reservoirs are developed in the western sag of the Lucaogou Formation in Jimusar. Favorable conditions for unconventional oil are formed here, and the resource potential is great.

DATA AVAILABILITY STATEMENT

The original contributions presented in the study are included in the article/Supplementary Material, further inquiries can be directed to the corresponding author.

AUTHOR CONTRIBUTIONS

HX designed the project and wrote the main article. CA and ZD help to draw the figures and to draft the article. DX defined the statement of problem. JY help to discuss the main idea and help to draft the article. GD and PY help to calculate the data and draw the figures. JZ help to revise the figures. All authors reviewed the article.

FUNDING

This study was partly funded by the National Natural Science Foundation of China (No. 42072160).

REFERENCES

Cao, H., Zou, Y.-R., Lei, Y., Xi, D., Wan, X., and Peng, P. a. (2017a). Shale Oil Assessment for the Songliao Basin, Northeastern China, Using Oil Generation-Sorption Method. *Energy Fuels* 31, 4826–4842. doi:10.1021/acs.energyfuels.7b00098

Cao, Z., Liu, G., Xiang, B., Wang, P., Niu, G., Niu, Z., et al. (2017b). Geochemical Characteristics of Crude Oil from a Tight Oil Reservoir in the Lucaogou Formation, Jimusar Sag, Junggar Basin. *Bulletin* 101 (1), 39–72. doi:10.1306/05241614182

Clarkson, C. R., Solano, N., Bustin, R. M., Bustin, A. M. M., Chalmers, G. R. L., He, L., et al. (2013). Pore Structure Characterization of North American Shale Gas Reservoirs Using USANS/SANS, Gas Adsorption, and Mercury Intrusion. *Fuel* 103, 606–616. doi:10.1016/j.fuel.2012.06.119

Downare, T. D., and Mullins, O. C. (1995). Visible and Near-Infrared Fluorescence of Crude Oils. *Appl. Spectrosc.* 49 (6), 754–764. doi:10.1366/0003702953964462

Everett, D. H. (1972). IUPAC Manual of Symbols and Terminology", Appendix 2, Part 1, Colloid and Surface Chemistry. *Pure Appl. Chem.* 31, 578–621. doi:10.1351/pac197231040577

Guo, X., Shen, Y., and He, S. (2015). Quantitative Pore Characterization and the Relationship between Pore Distributions and Organic Matter in Shale Based on Nano-CT Image Analysis: a Case Study for a Lacustrine Shale Reservoir in the Triassic Chang 7 Member, Ordos Basin, China. *J. Nat. Gas Sci. Eng.* 27 (3), 1630–1640. doi:10.1016/j.jngse.2015.10.033

He, C. Z., and Hua, M. Q. (1998). Fractal Geometry Description of Reservoir Pore Structure. *Oil Gas Geology.* 19, 15–23.

He, T., Li, W., Lu, S., Pan, W., Ying, J., Zhu, P., et al. (2022). Mechanism and Geological Significance of Anomalous Negative δ13Ckerogen in the Lower Cambrian, NW Tarim Basin, China. *J. Pet. Sci. Eng.* 208, 109384. doi:10.1016/j.petrol.2021.109384

He, T., Lu, S., Li, W., Tan, Z., and Zhang, X. (2018). Effect of Salinity on Source Rock Formation and its Control on the Oil Content in Shales in the Hetaoyuan Formation from the Biyang Depression, Nanxiang Basin, Central China. *Energy Fuels* 32 (6), 6698–6707. doi:10.1021/acs.energyfuels.8b01075

Hu, T., Pang, X., Jiang, S., Wang, Q., Zheng, X., Ding, X., et al. (2018). Oil Content Evaluation of Lacustrine Organic-Rich Shale with strong Heterogeneity: A Case Study of the Middle Permian Lucaogou Formation in Jimusaer Sag, Junggar Basin, NW China. *Fuel* 221, 196–205. doi:10.1016/j.fuel.2018.02.082

Huang, F. X., Yang, T., and Yan, W. P. (2013). *Geologic Factors of Formation of Tight Oil and its Resource Potential in China*. Pennsylvania: AAPG Annual Convention and Exhibition Pitsburgh.

Jarvie, D. M. (2012). Shale Resource Systems for Oil and Gas: Part 2—Shale-Oil Resource Systems. *AAPG Memoir* 97, 89–119. doi:10.1306/13321447M973489

Jiang, C., Chen, Z., Mort, A., Milovic, M., Robinson, R., Stewart, R., et al. (2016). Hydrocarbon Evaporative Loss from Shale Core Samples as Revealed by Rock-Eval and thermal Desorption-Gas Chromatography Analysis: Its Geochemical and Geological Implications. *Mar. Pet. Geology* 70, 294–303. doi:10.1016/j.marpetgeo.2015.11.021

Jiao, F., Zou, C., and Yang, Z. (2020). Geological Theory and Exploration & Development Practice of Hydrocarbon Accumulation inside continental Source Kitchens. *Pet. Exploration Dev.* 47 (6), 1147–1159. doi:10.3969/j.issn.1672-7703.2018.04.009

Kuang, L., Tang, Y., Lei, D., Chang, Q., Ouyang, M., Hou, L., et al. (2012). Formation Conditions and Exploration Potential of Tight Oil in the Permian saline Lacustrine Dolomitic Rock, Junggar Basin, NW China. *Pet. Exploration Dev.* 39 (6), 700–711. doi:10.1016/S1876-3804(12)60095-0

Li, J., Jiang, C., Wang, M., Lu, S., Chen, Z., Chen, G., et al. (2020). Adsorbed and Free Hydrocarbons in Unconventional Shale Reservoir: A New Insight from NMR T1-T2 Maps. *Mar. Pet. Geology* 116, 104311. doi:10.1016/j.marpetgeo.2020.104311

Li, J., Liu, D., Yao, Y., Cai, Y., and Guo, X. (2013). Physical Characterization of the Pore-Fracture System in Coals, Northeastern China. *Energy Exploration & Exploitation* 31 (2), 267–285. doi:10.1260/0144-5987.31.2.267

Li, J., Lu, S., Chen, G., Wang, M., Tian, S., and Guo, Z. (2019). A New Method for Measuring Shale Porosity with Low-Field Nuclear Magnetic Resonance Considering Non-fluid Signals. *Mar. Pet. Geology.* 102, 535–543. doi:10.1016/j.marpetgeo.2019.01.013

Li, W., Lu, S., Li, J., Wei, Y., Feng, W., Zhang, P., et al. (2021). Geochemical Modeling of Carbon Isotope Fractionation during Methane Transport in Tight Sedimentary Rocks. *Chem. Geology.* 566, 120033. doi:10.1016/j.chemgeo.2020.120033

Li, W., Lu, S., Xue, H., Zhang, P., and Hu, Y. (2015). Oil Content in Argillaceous Dolomite from the Jianghan Basin, China: Application of New Grading Evaluation Criteria to Study Shale Oil Potential. *Fuel* 143 (1), 424–429. doi:10.1016/j.fuel.2014.11.080

Lin, M., Xi, K., Cao, Y., Liu, Q., Zhang, Z., and Li, K. (2021). Petrographic Features and Diagenetic Alteration in the Shale Strata of the Permian Lucaogou Formation, Jimusar Sag, Junggar Basin. *J. Pet. Sci. Eng.* 203, 108684. doi:10.1016/j.petrol.2021.108684

Liu, B., Bai, L., Chi, Y., Jia, R., Fu, X., and Yang, L. (2019). Geochemical Characterization and Quantitative Evaluation of Shale Oil Reservoir by Two-Dimensional Nuclear Magnetic Resonance and Quantitative Grain Fluorescence on Extract: A Case Study from the Qingshankou Formation in Southern Songliao Basin, Northeast China. *Mar. Pet. Geology.* 109, 561–573. doi:10.1016/j.marpetgeo.2019.06.046

Liu, B., Wang, H., Fu, X., Bai, Y., Bai, L., Jia, M., et al. (2019). Lithofacies and Depositional Setting of a Highly Prospective Lacustrine Shale Oil Succession from the Upper Cretaceous Qingshankou Formation in the Gulong Sag, Northern Songliao Basin, Northeast China. *Bulletin* 103 (2), 405–432. doi:10.1306/08031817416

Liu, K., and Eadington, P. (2005). Quantitative Fluorescence Techniques for Detecting Residual Oils and Reconstructing Hydrocarbon Charge History. *Org. Geochem.* 36 (7), 1023–1036. doi:10.1016/j.orggeochem.2005.02.008

Loucks, R. G., Reed, R. M., Ruppel, S. C., and Hammes, U. (2012). Spectrum of Pore Types and Networks in Mudrocks and a Descriptive Classification for Matrix-Related Mudrock Pores. *Bulletin* 96 (6), 1071–1098. doi:10.1306/08171111061

Lu, S., Huang, W., Chen, F., Li, J., Wang, M., Xue, H., et al. (2012). Classification and Evaluation Criteria of Shale Oil and Gas Resources: Discussion and Application. *Pet. exploration Dev.* 39 (2), 268–276. doi:10.1016/s1876-3804(12)60042-1

Lu, S., Li, J., Zhang, P., Xue, H., Wang, G., Zhang, J., et al. (2018). Classification of Microscopic Pore-Throats and the Grading Evaluation on Shale Oil Reservoirs. *Pet. Exploration Dev.* 45 (3), 452–460. doi:10.1016/S1876-3804(18)30050-8

Mount, J. F. (1984). Mixing of Siliciclastic and Carbonate Sediments in Shallow Shelf Environments. *Geol.* 12 (7), 432–435. doi:10.1130/0091-7613(1984)12<432:mosacs>2.0.co;2

Odusina, E., Sondergeld, C., and Rai, C. (2011). An NMR Study on Shale Wettability. in Canadian Unconventional Resources Conference, Calgary, Alberta, Canada, November 2011. doi:10.2118/147371-ms

Pang, H., Pang, X.-q., Dong, L., and Zhao, X. (2018). Factors Impacting on Oil Retention in Lacustrine Shale: Permian Lucaogou Formation in Jimusaer Depression, Junggar Basin. *J. Pet. Sci. Eng.* 163, 79–90. doi:10.1016/j.petrol.2017.12.080

Plint, A. G., MacQuaker, J. H. S., and Varban, B. L. (2012). Bedload Transport of Mud across A Wide, Storm-Influenced Ramp: Cenomanian-Turonian Kaskapau Formation, Western Canada Foreland Basin. *J. Sediment. Res.* 82 (12), 801–822. doi:10.2110/jsr.2012.64

Qiu, Z., Tao, H., Zou, C., Wang, H., Ji, H., and Zhou, S. (2016). Lithofacies and Organic Geochemistry of the Middle Permian Lucaogou Formation in the Jimusar Sag of the Junggar Basin, NW China. *J. Pet. Sci. Eng.* 140, 97–107. doi:10.1016/j.jseaes.2018.08.021

Schieber, J. (1990). Significance of Styles of Epicontinental Shale Sedimentation in the Belt Basin, Mid-proterozoic of Montana. *USA. Sediment. Geol.* 69 (3), 297–312. doi:10.1016/0037-0738(90)90055-X

Slatt, R. M., and Rodriguez, N. D. (2012). Comparative Sequence Stratigraphy and Organic Geochemistry of Gas Shales: Commonality or Coincidence?. *J. Nat. Gas Sci. Eng.* 8, 68–84. doi:10.1016/j.jngse.2012.01.008

Song, Y., Luo, Q., Jiang, Z., Yang, W., and Liu, D. (2021). Enrichment of Tight Oil and its Controlling Factors in central and Western China. *Pet. Exploration Dev.* 48 (2), 492–506. doi:10.1016/S1876-3804(21)60040-X

Tian, H., Pan, L., Xiao, X., Wilkins, R. W. T., Meng, Z., and Huang, B. (2013). A Preliminary Study on the Pore Characterization of Lower Silurian Black Shales in the Chuandong Thrust Fold Belt, Southwestern China Using Low Pressure N2 Adsorption and FE-SEM Methods. *Mar. Pet. Geology.* 48, 8–19. doi:10.1016/j.marpetgeo.2013.07.008

Tian, S., Bowen, L., Liu, B., Zeng, F., Xue, H., Erastova, V., et al. (2021). A Method for Automatic Shale Porosity Quantification Using an Edge-Threshold Automatic Processing (ETAP) Technique. *Fuel* 304, 121319. doi:10.1016/j.fuel.2021.121319

Wang, E., Feng, Y., Liu, G., Chen, S., Wu, Z., and Li, C. (2021). Hydrocarbon Source Potential Evaluation Insight into Source Rocks-A Case Study of the First Member of the Paleogene Shahejie Formation, Nanpu Sag, NE China. *Energ. Rep.* 7, 32–42. doi:10.1016/j.egyr.2020.11.099

Wang, E., Liu, G., Pang, X., Li, C., Zhao, Z., Feng, Y., et al. (2020). An Improved Hydrocarbon Generation Potential Method for Quantifying Hydrocarbon Generation and Expulsion Characteristics with Application Example of Paleogene Shahejie Formation, Nanpu Sag, Bohai Bay Basin. *Mar. Pet. Geology.* 112, 104106. doi:10.1016/j.marpetgeo.2019.104106

Wang, G., and Ju, Y. (2015). Organic Shale Micropore and Mesopore Structure Characterization by Ultra-low Pressure N 2 Physisorption: Experimental Procedure and Interpretation Model. *J. Nat. Gas Sci. Eng.* 27 (2), 452–465. doi:10.1016/j.jngse.2015.08.003

Wang, J. G., Zhang, D. W., Yuan, J. Y., Li, X., Huang, C. G., and Shi, Y. J. (2019). Characteristics of Reservoir Genesis and Oil-Gas Accumulation in Lacustrine Carbonate in Yingxi Area of Qaidam Basin. *J. China Univ. Mining Tech.* 48 (1), 110–119. doi:10.13247/j.cnki.jcumt.000873

Xiao, D., Gao, Y., Peng, S., Wang, M., Wang, M., and Lu, S. (2021). Classification and Control Factors of Pore-Throat Systems in Hybrid Sedimentary Rocks of Jimusar Sag, Junggar Basin, NW China. *Pet. Exploration Dev.* 48 (4), 835–849. doi:10.1016/S1876-3804(21)60070-8

Xu, L., Chang, Q. S., Yang, K. C., Tao, Q., Wang, S., Fei, L., et al. (2019). Characteristics and Oil-Bearing Capability of Shale Oil Reservoir in the Permian Lucaogou Formation, Jimusar Sag. *Oil Gas Geology.* 40 (3), 536–540. doi:10.11743/ogg20190309

Yang, Y., Qiu, L., Wan, M., Jia, X., Cao, Y., Lei, D., et al. (2019). Depositional Model for a Salinized Lacustrine basin: The Permian Lucaogou Formation, Jimsar Sag, Junggar Basin, NW China. *J. Asian Earth Sci.* 178, 81–95. doi:10.1016/j.jseaes.2018.08.021

Yang, Z., Hou, L. H., Lin, S. H., Luo, X., Zhang, L. J., Wu, S. T., et al. (2018). Geologic Characteristics and Exploration Potential of Tight Oil and Shale Oil in Lucaogou Formation in Jimsar Sag. *China Pet. Exploration* 23 (4), 76–85. doi:10.3969/j.issn.1672-7703.2018.04.009

Zeng, F., Dong, C. M., Lin, C. Y., Tian, S. S., Wu, Y. Q., Lin, J. L., et al. (2021a). Pore Structure Characteristics of Reservoirs of Xihu Sag in East China Sea Shelf Basin Based on Dual Resolution X-Ray Computed Tomography and Their Influence on Permeability. *Energy*, 122386. doi:10.1016/j.energy.2021.122386

Zeng, F., Dong, C. M., Lin, C. Y., Wu, Y. Q., Tian, S. S., Zhang, X. G., et al. (2021b). Analyzing the Effects of Multi-Scale Pore Systems on Reservoir Properties—A Case Study on Xihu Depression, East China Sea Shelf Basin, China. *J. Pet. Sci. Eng.* 203, 108609. doi:10.1016/j.petrol.2021.108609

Zhang, J., Liu, G., Cao, Z., Tao, S., Felix, M., Kong, Y., et al. (2019). Characteristics and Formation Mechanism of Multi-Source Mixed Sedimentary Rocks in a saline lake, a Case Study of the Permian Lucaogou Formation in the Jimusaer Sag, Northwest China. *Mar. Pet. Geology.* 102, 704–724. doi:10.1016/j.marpetgeo.2019.01.016

Zhang, P., Lu, S., Li, J., Xue, H., Li, W., and Zhang, P. (2017). Characterization of Shale Pore System: a Case Study of Paleogene Xin'gouzui Formation in the Jianghan basin, China. *Mar. Pet. Geology.* 79, 321–334. doi:10.1016/j.marpetgeo.2016.10.014

Zhang, S. M., Cao, Y. C., Zhu, R. K., Xi, K. L., Wang, J., Zhu, N., et al. (2018). Lithofacies Classification of fine-grained Mixed Sedimentary Rocks in the Permain Lucaogou Formation, Jimsar Sag, Junggar Basin. *Earth Sci. Front.* 25 (4), 198–209. doi:10.13745/j.esf.yx.2017-5-2

Zhang, Y. Q., Ma, S. Z., Gao, Y., Li, Y., Zhang, J., Wang, L., et al. (2017). Depositional Facies Analysis on Tight Reservoir of Lucaogou Formation inJimusar Sag. *Acta Sedimentol Sinica* 35 (2), 358–370. doi:10.14027/j.cnki.cjxb.2017.02.013

Zhao, J. H., Jin, Z. J., Jin, Z. K., Wen, X., Geng, Y. K., Yan, C. N., et al. (2016). Lithofacies Types and Sedimentary Environment of Shale in Wufeng-Longmaxi Formation, Sichuan Basin. *Acta Petrolei Sinica* 37 (5), 572–586. doi:10.7623/syxb201605002

Zou, C., Yang, Z., Zhang, G., Hou, L., Zhu, R., Tao, S., et al. (2014). Conventional and Unconventional Petroleum "Orderly Accumulation": Concept and Practical Significance. *Pet. Exploration Dev.* 41 (1), 14–30. doi:10.1016/S1876-3804(14)60002-1

Conflict of Interest: The authors declare that the research was conducted in the absence of any commercial or financial relationships that could be construed as a potential conflict of interest.

Publisher's Note: All claims expressed in this article are solely those of the authors and do not necessarily represent those of their affiliated organizations, or those of the publisher, the editors and the reviewers. Any product that may be evaluated in this article, or claim that may be made by its manufacturer, is not guaranteed or endorsed by the publisher.